Desalination and Water Treatment
www.deswater.com
doi: 10.5004/dwt.2019.23898

152 (2019) 383–392
June

Ag: ZrO_2-NPs-AC based nanocomposite as a novel sorbent for trapping hazardous food additive dye from water sample

Marjan Moradi[a], Nahid Rastakhiz[a,*], Mehrorang Ghaedi[b], Rahele Zhiani[c]

[a]*Department of Chemistry, Kerman Branch, Islamic Azad University, Kerman, Iran, Tel./Fax: +98-3432476934; emails: nahid.rastakhiz@yahoo.com (N. Rastakhiz), marjanmoradi86@yahoo.com (M. Moradi)*
[b]*Chemistry Department, Yasouj University Yasouj, Iran, email: m_ghaedi@yahoo.com*
[c]*Department of Chemistry, Nyshabur Branch, Islamic Azad University, Nyshabur, Iran, email: r_zhiani2006@yahoo.com*

Received 7 July 2018; Accepted 1 February 2019

ABSTRACT

This study aimed at pre-concentrating Allura Red as a food additive dye and determining it in the environmental samples following its extraction. Dispersive solid-phase extraction was followed by UV–Vis spectroscopy to provide a simple and efficient method with low cost by using silver-zirconium oxide nanoparticles loaded on an activated carbon as the adsorbent. The proposed adsorbent was simply prepared and characterized by different techniques, such as Fourier-transform infrared spectroscopy, X-ray diffraction, and scanning electron microscopy. Evaluation and optimization of the effective parameters on the extraction recovery, including eluent volume (mL), pH, adsorbent dosage (mg), and ultrasound time (min), and their interactions were investigated using a response surface methodology based on a central composite design as an efficient mathematical and statistical tool. The selected model›s precision and accuracy were assessed through the analysis of variance, while the optimum conditions were obtained as follows: eluent volume = 0.3 mL, pH = 3, adsorbent dosage = 10 mg, and ultrasound time = 4.5 min. Under the optimum operational conditions, the limit of quantification of 75.0 ng mL^{-1}, limit of detection of 26.0 ng mL^{-1}, and linear range of 80.0–5,000 ng mL^{-1} were achieved. A high correlation coefficient was obtained via the Langmuir isotherm as best model, from which the maximum adsorption capacity of 52.40 mg g^{-1} was resulted.

Keywords: Allura Red; Dispersive solid phase extraction; Nanostructured adsorbent; Environmental samples; Response surface methodology

1. Introduction

Synthetic food dyes account for one of the most important classes of food additives that have been widely utilized in different food industries. They are usually added to food stuffs, soft drinks, candies, and chocolates to improve their appearances, colors, textures, tastes, nutritive values, and protections and thus make them more attractive to customers [1]. Although these dyes are highly applicable, some of them can be pathogenic and hence not recommended. Therefore, investigation and monitoring of these chemical dyes for their toxicities and/or side effects are so vital for researchers to be finally encouraged to design and develop valid analytical methods for their rapid and accurate extractions and determinations [2,3].

AR (Fig. 1) is a synthetic food additive dye, which is used in many commercial food products, such as gelatins, puddings, ice cream, drinks, and other foods [4]. Its aromatic ring structure and azo (N=N) functional group can not only affect human and animal health, but also cause hyperactivity in children. Hence, its detection and determination are extremely important [5]. Different methods, such as high-performance liquid chromatography (HPLC) [6], capillary electrophoresis, gas chromatography/mass spectrometry (GC/MS), liquid chromatography/mass spectrometry (LC/MS), liquid chromatography/tandem mass spectrometry

* Corresponding author.

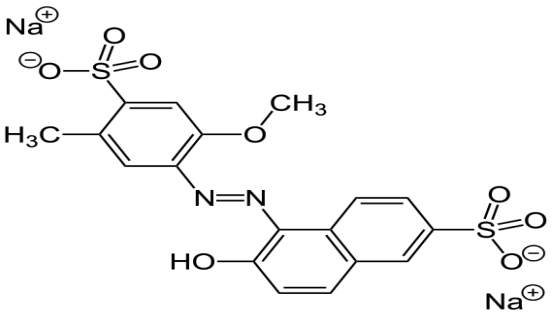

Fig. 1. Chemical structure of Allura Red.

(LC/TMS) [7], high-performance liquid chromatography/mass spectrometry (HPLC/MS), voltammetry, electrochemical method, and UV–Vis spectroscopy, have been applied for the determination of synthetic food dyes. Among them, UV–Vis spectroscopy is an appropriate approach to the analysis of organic compounds, especially organic food dyes due to its low cost, high sensitivity, great accessibility, short analysis time, and easy operation [8]. Although UV–Vis spectroscopy has very important advantages, direct analyses of crude samples are not usually suggested due to the presence of complex sample matrices and low analyte concentrations that can affect the physical and chemical properties of analyte. Hence, accurate analyte quantification requires taking effective steps for sample preparation prior to instrumental analysis [9]. The two main objectives of sample preparation include elimination of matrix interferences and/or analyte pre-concentrations [10].

Liquid–liquid extraction [11] and solid–phase extraction (SPE) [12] are two most applicable pretreatment methods preliminarily used for the pre-concentration and determination of synthetic food dyes. However, they are time-consuming and sometimes laborious apart from their unique merits and advantages. For the mentioned reasons, researchers may be encouraged to turn to the other techniques, that is, DSPE [13–16] micro-solid-phase extraction (MSPE), and dispersive solid-phase micro-extraction (DSPME) [17]. DSPE is based on the adsorbent dispersion in a liquid sample. Thus, it not only prevents the adsorbent from retaining in the cartridge, disk, or needle, but also avoids channeling or blocking of cartridges or disks despite the traditional SPE methods. On the other hand, contrary to the conventional SPE, the adsorbent preconditioning is not necessary in DSPE, the performance of which can be simplified and the extraction time can be reduced without a decrease in its effectiveness and efficiency [18]. In the DSPE procedure, various adsorbents are utilized. Selection of an appropriate adsorbent is very crucial for the efficient extraction of the target analyte. Nanostructured adsorbents have been widely employed for the pre-concentration of analyte due to their advantages of unique physical [3], chemical, and biological properties [19], high surface areas, and short diffusion routes, which can result in high adsorption capacity and efficiency [20,21], as well as fast extraction kinetics [22,23]. Nanoparticle-based adsorbents are chemically more reactive than larger particles. Among the inorganic nanoparticles, silver has been recognized as an effective antimicrobial agent, which exhibits a low toxicity in humans and has a high surface area-to-volume ratio [24,25]. Zirconia (ZrO_2) nanoparticles (ZNPs) have especially interested researchers in this field due to their high surface area-to-volume ratio, thermal stability, chemical inertness, and lack of toxicity [26]. On the other hand, activated carbon has been turned out to be an effective adsorbent for the extraction of different analyte due to its high surface area, wide range of surface functional groups, and internal microporosity [27]. Therefore, these specific and distinguished properties of nanostructures encourage researchers to use them as reliable adsorbents based on DSPE approach. Since the extraction of food dyes is influenced by various parameters, a different approach has been applied by researchers to efficiently, rapidly, and accurately identify optimal conditions [13].

RSM based on a CCD provides one of the most effective mathematical and statistical tools for the optimization of multifaceted processes and evaluation of the effects of multiple variables and their interactions [28–32]. It consists of a group of mathematical and statistical techniques that are based on the fitness of empirical models to the experimental data obtained in relation to an experimental design [33–36]. Among the effective parameters on extraction recovery, ultrasound waves can efficiently increase the extraction recoveries of analyte. During the propagation of ultrasonic waves, cavitation bubbles capable of shearing the created force are generated. On the other hand, the collapse of the bubbles leads to enhanced homogeneity of the solution, thereby increasing the releases of extractable compounds. Therefore, ultrasound waves can raise homogeneity of solutions and mass transfer of analyte, which would extensively accelerate analyte separation and extraction [37].

In this study, DSPE-based Ag:ZrO_2–AC nanostructured adsorbent was used followed by UV–Vis spectrophotometry as a miniaturized, simple, rapid, and efficient method for AR extraction and determination. Ag:ZrO_2–NPs–AC as an efficient adsorbent was simply prepared and investigated via different techniques. Also, for the analysis and optimization of the main parameters, an RSM-based CCD was applied. Then, the method performance was evaluated in terms of limit of detection (LOD) and limit of quantification (LOQ) values, linearity (LR), precision, repeatability, and accuracy under optimal conditions.

2. Experimental

2.1. Standard solutions and chemical reagents

After purchasing $AgNO_3$, $NaBH_4$, NH_3, NaOH, HCl, and some other reagents from Sigma-Aldrich Company (St. Louis, MO, USA) and activated carbon from Merck Company (Darmstadt, Germany), we used them without any further purification. All the other chemicals were of analytical grade. Preparations of the solutions in distilled water were followed. After the daily preparation of 100 mg L^{-1} of AR stock solutions in deionized water, they were diluted with deionized water to obtain proper concentration to establish the calibration curve based on the standard solutions.

2.2. Instrumental characterization and software

All the absorbance measurements were performed with the help of a dual beam UV–Vis spectrophotometer

(Model Lambda 25, PerkinElmer, USA) with a 1 cm susceptibility-matched microcell. An ultrasonic bath system (TECNO-GAZ, Parma, Italy) at 40 kHz of frequency was applied for the analyte extraction. A pH-meter (Metrohm 686, Switzerland) was employed to adjust the pH values using a combined glass electrode. An ultrasonic bath with heating system (Techno-GAZ SPA Ultra Sonic System) at 40 kHz of frequency and 130 W of power was used for the ultrasound-assisted adsorption. The adsorbent characterization was carried out using a Fourier transform infrared spectrometer (FT-IR-8300, Shimadzu, Japan). KBr pellets were utilized for the identification of functional groups with the help of a scanning electron microscope (Hitachi S4160, Tokyo, Japan) and an X-ray diffractometer (Philips PW1800, the Netherland). Finally, the statistical "Design-Expert" software package (version 7.0, Stat-Ease Inc., Minneapolis, USA) was used for the optimizations through the statistical analyses and model-fitting based on the 3D plots.

2.3. Preparation of ZrO_2–NPs–AC

For the preparation of ZrO_2–NP–AC, 250 mL of the dispersed ZrO_2 NP suspension (0.25 g L^{-1}) was mixed with activated carbon (5 g) in a 500 mL flask under magnetic stirring for 24 h, which led to the deposition of ZrO_2 NPs on the activated carbon. ZrO_2–NP–AC was then filtered and extensively washed with distilled water. It was generally dried at 100°C overnight. A mortar was utilized to homogeneously grind the ZrO_2–NP–AC.

2.4. Preparation of Ag-embedded ZrO_2–NPs–AC

For the preparation of Ag-embedded ZrO_2–NPs–AC, 2 g of ZrO_2–NP–AC powder was soaked in 40 mL of $AgNO_3$ (1 M) solution. After 24 h of impregnation in the dark, the powder sample was washed with water to remove the loosely adsorbed $AgNO_3$ until no $AgNO_3$ was observed in the filtrate. Thus, the retention of only strongly adsorbed $AgNO_3$ within ZrO_2–NPs–AC was ensured. The powder samples collected on the filter paper were dried in a vacuum desiccator. In the second step, 1 g of ZrO_2–NPs–AC was immersed in 5 mL of 0.2 M $NaBH_4$ solution for 24 h at room temperature to allow the formation of Ag particles. Then, excess $NaBH_4$ was removed by washing it with water and drying it again [38].

2.5. Dispersive solid-phase extraction procedure

15 mL of the sample was transferred into a glass centrifuge tube and its pH was adjusted at the desired value of 4 with 0.1 mol L^{-1} of HCl and/or NaOH solution. Then, 8 mg of Ag:ZrO_2–NPs–AC adsorbent was added to the mentioned solution. The adsorption process was facilitated by transferring the prepared solution to an ultrasound bath (40 kHz, 6 frequency and 0.130 kW of power at 25°C) for 3 min. Ag:ZrO_2–NPs–AC was separated from the solution by centrifuging the adsorbed analyte at 5,000 rpm for 3 min. Discarding of the upper water phase was followed by dissolving the analyte in 300 μL of tetrahydrofuran (THF) in the ultrasonic bath at 25°C for 1 min and centrifuging it at 5,000 rpm for 3 min. Ultimately, AR absorbance intensities (λ_{max}) were determined at 520 nm after transferring a proper amount of the obtained solution into the spectrophotometric microcell.

3. Results and discussion

3.1. Characterization of Ag:ZrO_2–NPs–AC adsorbent

The structure and morphology of Ag:ZrO_2–NPs–AC were investigated using different techniques, such as FT-IR spectroscopy, XRD, and SEM. The FT-IR spectrum of Ag:ZrO_2–AC is shown in Fig. 2. As depicted in this figure, the strong characteristic absorption peak at 3,445 cm^{-1} is assigned to the stretching vibration of water molecules [39]. In addition, O–H bending vibration at 1,592 cm^{-1} has been presented. Also, the bands at 509 and 746 cm^{-1} are attributed to the stretching vibration of Zr–O [40]. The possible interaction between silver and oxygen-containing groups was further confirmed by the appearance of a new band at approximately 520 cm^{-1} corresponding to the stretching vibration of Ag–O group [41]. The XRD pattern of Ag:ZrO_2–AC is shown in Fig. 3. The XRD pattern of Ag:ZrO_2–AC displays three characteristic peaks at 2θ values of 38.03°, 44.22°, and 64.45° corresponding to the (111), (200), and (220) crystalline planes of Ag crystal, respectively. Also, the peaks found at 2θ = ~27.05° and 55° originate from the monoclinic ZrO_2 planes of (111) and (202), respectively [42]. On the other hand, the broad hump at 2θ = 17–25 and peak at 2θ = 42 are corresponding to the (002) and (101) planes of the amorphous activated carbon modified with Ag:ZrO_2 nanoparticles, respectively [39]. Fig. 4 depicts the SEM image of Ag:ZrO_2–AC confirming the homogeneous distribution of Ag:ZrO_2 nanoparticles on the activated carbon.

3.2. Effect of extraction solvent

For AR desorption from Ag:ZrO_2–AC, different eluent solvents, such as tetrahydrofuran (THF), dimethylformamide (DMF), methanol (MeOH), acetonitrile (AN), acetone (AC), and ethanol (EtOH) were applied at the following conditions: (concentration of AR: 250 ng mL^{-1}, pH: 4, solution volume: 10 mL, adsorbent dosage: 8 mg, sonication time: 3 min and eluent volume: 200 μL). Among tested eluents, THF had maximum efficiency for AR desorption from the adsorbent due to its strongest dissolving ability of AR.

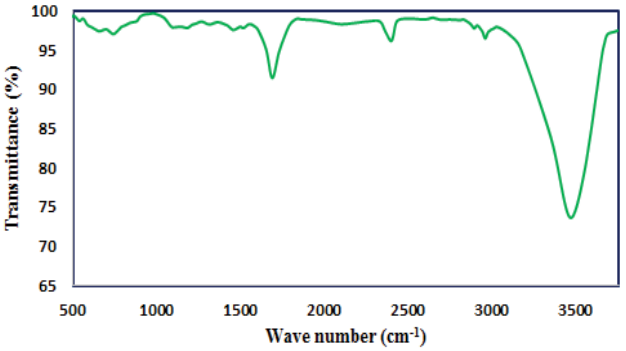

Fig. 2. FT-IR spectra of Ag:ZrO_2–AC.

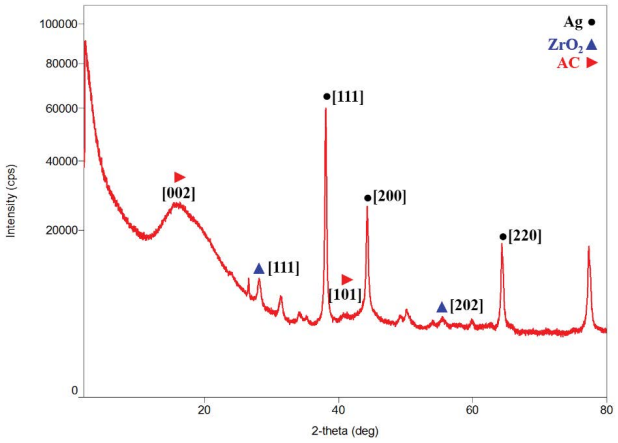

Fig. 3. XRD pattern of Ag:ZrO_2–AC.

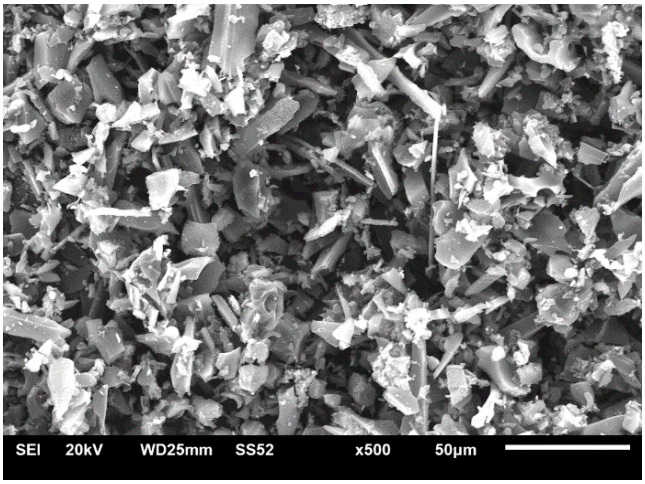

Fig. 4. SEM image of Ag:ZrO_2–AC.

3.3. Evaluation of effective parameters by CCD based RSM

CCD-based RSM is an effective mathematical and statistical tool that can be used to evaluate the effects of effective parameters and their interactions on extraction recovery and thus optimize the selected parameters [43]. "Design-Expert Software", version 7 was applied for this purpose. Eluent volume (mL) (*A*), pH (*B*), adsorbent dosage (mg) (*C*), and ultrasound time (min) (*D*) as the effective factors on the extraction recovery were considered at five levels ($-\alpha$, −1, 0, 1, and $+\alpha$). The experimental factors, levels, values, and responses are shown in Table 1. The experimental results were fitted with the full quadratic model by using a multiple regression technique as follows:

$$\mathrm{ER}\% = +81.33 + 2.14A - 5.00B + 5.66C + 8.3D + 6.71AB - 3.18AD - 3.73A^2 + 0.83B^2 - 2.78D^2 \quad (1)$$

where *Y* is a response variable for AR determination. The acceptable quality of the polynomial model fit could be expressed by the coefficients of determination (R^2 = 0.9969 and adjusted R^2 = 0.9883). The plot of the observed (%) vs. predicted values confirmed a good fit (Fig. 5). A summary of the results of the analysis of variance (ANOVA) obtained for the design matrix is presented in Table 2. The model's adequacy and significance, as well as the factors and their interactions were utilized based on *P* and *F* values. Their significant contributions to the extraction process were strongly supported by the factors having the *p* values of less than 0.05. Contrarily, the factors with the *p* values of higher than 0.05 showed non-significant contributions to the model. As shown in Table 2, *A* (eluent volume), *B* (pH), *C* (adsorbent dosage), *D* (ultrasound time), *AB*, *AD*, A^2, B^2, and D^2 have the *p* values of less than 0.05, thus representing a significant contribution to the extraction process. Also, *AC*, *BC*, *BD*, *CD*, and C^2 with the *p* values of higher than 0.05 exhibit non-significant contributions to the extraction process. RSM was employed to optimize the critical factors and describe the nature of the response surface in the experiment. The relevant fitted response surfaces for the design and the response surface plots of the extraction (%) vs. significant variables are displayed in Fig. 6. These plots were obtained for a given pair of factors as the central values for the other variables. The curvatures of the plots indicated the interactions between the variables. Figs. 6(a) and (b) demonstrate the influence of the adsorbent dosage on AR recovery. The enhancement of AR extraction percentage by raising the adsorbent dosage is due to its high specific surface area and abundant reactive surface center. The significantly elevated adsorption rate at higher dosage values is probably due to an increase in the adsorbent surface area and availability of more active adsorption sites. The significantly enhanced of AR extraction percentage at lower amounts of the adsorbent has been caused by the insufficient reactive sites and higher ratio of AR molecules to vacant sites. Based on Figs. 6(b) and (d), the extraction percentage of AR increases by increasing the ultrasound time, which is due to the specific properties of ultrasound irradiations, such as shock waves, microjets, and high-velocity inter-particle collisions that can enhance both the contact surfaces of AR molecules and Ag:ZrO_2–AC and mass transfer through turbulent mixing. The effect of pH as one of the most effective factors on AR extraction recovery was investigated (Fig. 6(c)). It was seen to affect both the adsorbent surface properties and AR structure. The results were indicative of higher AR adsorption at acidic pH. At a low pH value, protons had a high concentration in the solution. These protons were adsorbed onto the adsorbent surface and generated a net positive charge on it. The electrostatic attraction force between the adsorbent and the anionic AR molecules could increase AR adsorption. On the other hand, the high concentration of the hydroxyl groups at lower pH values led to their adsorption onto the adsorbent surface and generation of a net negative charge on it. As a result of the electrostatic repulsion force between the adsorbent and anionic AR molecules, any higher AR removal was inhibited. It seemed that at pH 3 as the working medium, the two pathways of chemical reactions with zirconium, silver, oxygen atoms, and hydrogen bonding with various AC functional groups would accelerate AR adsorption onto Ag:ZrO_2–AC. The optimum extraction efficiency was achieved with 10 mg of Ag:ZrO_2–AC and 0.3 mL of THF at a pH value of 3 within 4.5 min of extraction time (Fig. 7).

Table 1
Experimental factors and levels in the central composite design for extraction of Allura Red

Factors	Unit	Code	−α	Levels			+α
				Low (−1)	Center (0)	High (+1)	
Eluent volume	mL	*A*	0.1	0.2	0.3	0.4	0.5
pH	–	*B*	3	4	5	6	7
Adsorbent dosage	mg	*C*	5	10	15	20	25
Ultrasound time	min	*D*	1	2	3	4	5

Run	Factors				ER% Allura Red		
	A	*B*	*C*	*D*	Experimental[a]	Predicted[b]	Residual
1	0.30	5.00	15.00	3.00	81.50	81.56	−0.60
2	0.20	6.00	20.00	4.00	79.50	78.77	0.73
3	0.20	4.00	10.00	2.00	67.20	67.45	−0.25
4	0.30	3.00	15.00	3.00	94.40	94.64	−0.24
5	0.40	6.00	10.00	2.00	69.00	69.25	−0.25
6	0.40	4.00	20.00	4.00	88.00	87.27	0.73
7	0.30	5.00	15.00	3.00	82.20	79.23	0.87
8	0.20	6.00	10.00	4.00	66.00	66.25	−0.25
9	0.30	5.00	25.00	3.00	90.70	91.92	−1.22
10	0.30	5.00	15.00	1.00	53.20	53.44	−0.24
11	0.20	4.00	20.00	2.00	78.90	78.17	0.73
12	0.10	5.00	15.00	3.00	61.87	62.11	−0.24
13	0.50	5.00	15.00	3.00	70.43	70.67	−0.24
14	0.40	4.00	10.00	4.00	76.00	76.25	−0.25
15	0.30	5.00	15.00	3.00	80.66	81.00	−0.34
16	0.30	5.00	15.00	3.00	80.94	81.33	−0.39
17	0.30	7.00	15.00	3.00	74.40	74.64	−0.24
18	0.40	6.00	20.00	2.00	81.00	80.27	0.73
19	0.30	5.00	15.00	5.00	86.73	86.97	−0.24
20	0.30	5.00	5.00	3.00	70.00	69.72	0.73

[a]Experimental values of response.
[b]Predicted values of response by RSM proposed model.

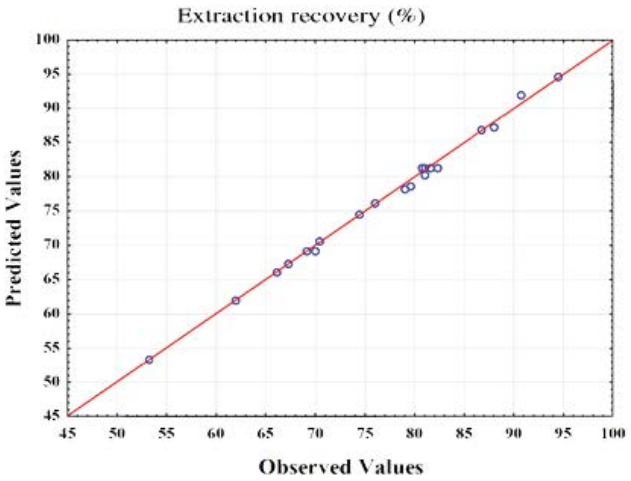

Fig. 5. Observed data vs. the predicted data of normalized extraction of Allura Red.

3.4. Validation of method

The results of studying the method's LOD, LOQ, linearity, repeatability, and reproducibility under the optimized conditions are calculated. The linear calibration curve appeared between 80 and 5,000 ng mL^{-1} with a correlation coefficient of 0.9984. LOD and LOQ were measured to be 3 and 10 S_b/m based on the equation, respectively. The relative standard deviations (RSDs %) of 1.0%–4.3% were obtained in four-replicate experiments (Table 3). The RSDs% of lower than 4.7% besides accuracy of 82.3%–93.6% represented as the mean recovery were strongly indicative of the successful applicability of the proposed approach in complex diluted matrices. These results revealed the excellent linearity, sensitivity, and reproducibility of combined Ag:ZrO_2–AC, DSPE, and UV–Vis for analyzing AR-containing food samples.

3.5. Interference

In this study, the effects of common interference species, such as metal ions and dyes on AR recovery using

Table 2
Analysis of variances for the response surface model of AR extraction

Source of variation	Sum of square	DF	Mean square	*F*-value	*P*-value
Model	1,975.67	14	141.12	115.19	<0.0001
A	36.64	1	36.64	29.91	0.0028
B	200.00	1	200.00	163.26	<0.0001
C	513.02	1	513.02	418.78	<0.0001
D	562.13	1	562.13	458.86	<0.0001
AB	179.96	1	179.96	146.90	<0.0001
AC	0.18	1	0.18	0.15	0.7172
AD	40.32	1	40.32	32.91	0.0023
BC	0.41	1	0.41	0.33	0.5902
BD	1.74	1	1.74	1.42	0.2865
CD	0.40	1	0.40	0.33	0.5902
A^2	324.36	1	324.36	264.77	<0.0001
B^2	16.00	1	16.00	13.06	0.0153
C^2	0.78	1	0.78	0.64	0.4606
D^2	179.80	1	179.80	146.77	<0.0001
Residual	6.13	5	1.23	115.19	<0.0001
Lack of fit	4.74	2	2.37		
Pure error	1.39	3	0.46	5.13	0.1077
Corrected total	1,981.80	19			
R^2	0.9969				
R^2-Adjust	0.9883				
R^2-Predicted	0.8665				

Ag:ZrO_2–AC was investigated. The results are given in Table 4. According to the data, some major matrix ions present in natural water samples have no obvious interferences and do not change the response more than ±5%. Heavy metal ions have less tolerable limits due to their competition and co-extraction. These ions had little interference with the DSPE-UV–Vis method probably due to low stabilities of their complex's with AR dye.

3.6. Adsorption capacity of Ag:ZrO_2–AC

The equilibrium adsorption isotherms have been widely used since they provide useful information about the

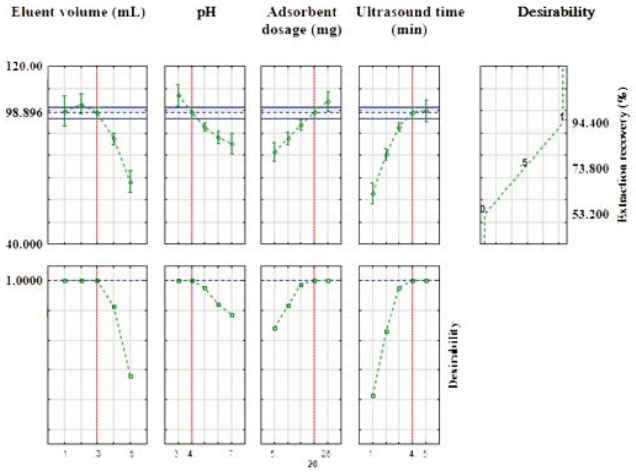

Fig. 7. Optimum and desirability functioned values for the extraction of Allura red.

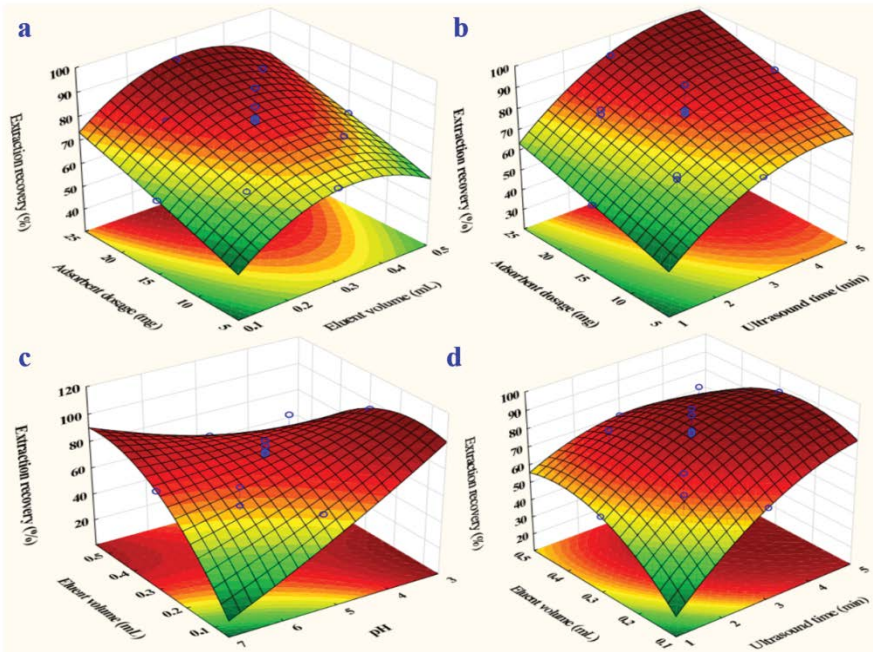

Fig. 6. Response surface showing Allura Red recovery efficiency as a function of two independent variables: (a) adsorbent dosage (mg) - eluent volume (mL), (b) adsorbent dosage (mg) - ultrasound time (min), (c) pH - adsorbent dosage (mg), and (d) ultrasound time (min) - eluent volume (mL) at 25°C.

Table 3
Precision of the Ag:ZrO_2–AC–DSPE-UV–Vis method (n = 4)

Inter-day			
Add	Found	RSD (%)	Related recovery (%)
80	61.7	3.8	77.2
500	460.0	4.1	92.0
2,000	1,780.0	3.6	99.9
4,000	3,730.0	2.8	93.2
Intra-day			
80	68.8	4.3	85.9
500	461.8	2.2	92.4
2,000	1,780.0	3.8	89.9
4,000	3,600.0	1.0	90.1

Table 4
Tolerance limits of interfering species in the extraction of AR dye (extraction conditions: water sample volume, 10.0 mL; sonication time, 4.5 min; pH, 3; eluent volume, 0.3 mL; adsorbent dosage, 10 mg; concentration of AR dye, 250 ng mL^{-1})

Interference	Tolerance ratio (mg L^{-1})
Cl^-, Na^+, K^+, I^-, NO_3^-, Ca^{2+}	600
Br^-, Ba^{2+}, Mg^{2+}	400
Fe^{3+}, Ni^{2+}	300
Ag^+, Co^{2+}, Pb^{2+}, Cr^{2+}	200
Tartrazine	300
Methylene blue	100

mechanism, properties, and tendency of an adsorbent toward each analyte. The data obtained during the equilibrium study were fitted to various adsorption isotherm equations, such as Langmuir and Freundlich so as to discuss the equilibrium characteristics of the adsorption process [44,45]. The adsorption isotherm and capacity of Ag:ZrO_2–AC were evaluated for AR extraction under the optimized conditions. In this regard, the Langmuir (Eq. (2)) and Freundlich (Eq. (3)) isotherms were applied based on our previous works [28].

$$\frac{C_e}{q_e} = \frac{1}{Q_m K_L} + \frac{C_e}{Q_m} \tag{2}$$

$$\ln q_e = \ln K_F + \frac{1}{n}\ln C_e \tag{3}$$

In this research, modeling of the experimental binding data was done based on the concentration range of 1–35 mg L^{-1}. The isotherms and parameters, respectively, obtained from the experimental data and nonlinear regression based on both models are shown in Fig. 8. The experimental data were better produced and explained by the Langmuir model whose R^2 (0.9936) was much larger than that of the Freundlich model (0.9572) and thus very close to 1. Also, the monolayer adsorption capacity (52.40 mg g^{-1}) of the former isotherm was seen to approach that of the experimental data (43.31 mg g^{-1}). This suggests that the mentioned isotherm governed AR sorption equilibrium onto Ag:ZrO_2–AC.

3.7. Assessment of proposed DSPE-UV–Vis method in real samples

Drinking and distilled water as real samples containing different AR values were used to evaluate the applicability

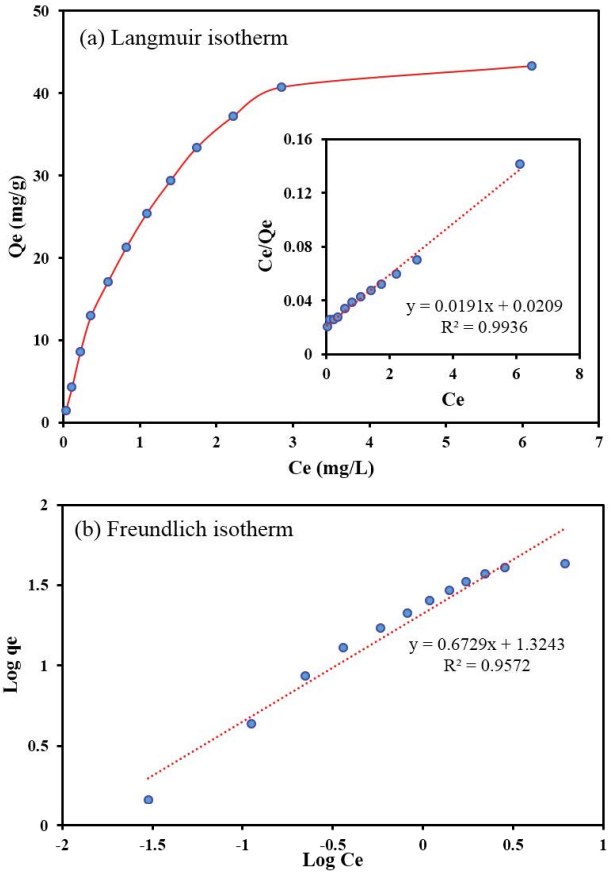

Fig. 8. Langmuir (a) and Freundlich (b) isotherm plots for the extraction of Allura Red adsorbed on Ag:ZrO_2–AC0.

Table 5
Accuracy of the Ag:ZrO_2–AC–DSPE-UV–Vis method (n = 3)

Inter-day			
Add	Found	RSD (%)	Related Recovery (%)
100	82.3	3.1	82.3
300	267.0	4.7	88.9
1,000	932.0	2.6	93.2
3,000	2,810.0	2.1	93.6
Intra-day			
100	89.0	4.0	89.0
300	273.0	2.6	91.0
1,000	840.0	2.4	84.0
3,000	2,763.0	1.7	92.0

Table 6
Comparison of DSPE-UV–Vis with other methods for determination of Allura red

Method	Detection	Linear range (ng mL^{-1})	LOD (ng mL^{-1})	LOQ (ng mL^{-1})	Ref
CPE[a]	UV–Vis[b]	400.0–8,000.0	120.0	330.0	[46]
SPE[c]	HPLC-DAD[d]	10,000.0–100,000.0	350.0	1,000.0	[47]
CE[e]	HPLC	2,000.0–10,000.0	59.0–102.0	198.0–341.0	[48]
MSPE[f]	HPLC-UV[g]	5.0–1,500.0	2.0	7.0	[49]
UA-D-μ-SPE[h]	HPLC-UV	1.0–5,000	0.198	0.659	[50]
CSPE[i]	UV–Vis	1,000.0–6,000.0	2.35	–	[51]
DSPE[j]	UV–Vis	80.0–5,000	26.0	75.0	Present work

[a]Cloud point extraction.
[b]Ultraviolet–Visible spectroscopy.
[c]Solid-phase extraction.
[d]High-performance liquid chromatography coupled with diode-array detector.
[e]Capillary electrophoresis.
[f]Magnetic solid-phase extraction.
[g]High-performance liquid chromatography-ultraviolet–visible detector.
[h]Ultrasound-assisted dispersive micro solid-phase extraction.
[i]Column solid-phase extraction-spectrophotometry.
[j]Dispersive solid-phase extraction.

of DSPE-UV–Vis method for AR determination in them. The final recoveries obtained from the extraction process under the optimized conditions were compared with those of the real samples, the results of which are summarized in Table 5. The accuracy values of 82.3%–93.6% were achieved through matrix-matched calibrations, whereas their respective RSD values showed to be lower than 4.7%. These findings confirmed the trivial impacts of the matrices of the mentioned samples on the proposed method's applicability to AR determination.

3.8. Desorption and reusability of Ag:ZrO_2–AC

The regeneration of Ag:ZrO_2–AC adsorbent is very vital for practical purposes. After each extraction experiment, the adsorbent was washed with 3 mL of THF and 3 mL of deionized water. The results confirmed the Ag:ZrO_2–AC can be reused at least four times in successive extraction processes without any significant losses in the sorption performance, which suggests the adsorbent stability during the elution stage.

3.9. Comparison of the DSPE-UV–Vis method with other methods

The performance of DSPE-UV–Vis method for determination of Allura red as a food additive dye was compared with some other reported in related literature (Table 6). As seen, present method has comparable linear range, LOD, and LOQ with other research works. Actually, a satisfactory linear range, LOD, and LOQ values were easily obtained via a good sample preparation procedure followed by simple, fast, and inexpensive instrumental analyses UV detector. Therefore, the proposed method offers a simple, cheap, and an acceptable procedure for the determination of Allura red from environmental samples using Ag:ZrO_2–NPs–AC nano-composite as an effective and novel sorbent.

4. Conclusion

Based on the aims of this study, Ag:ZrO_2–AC was synthesized in a simple and fast route and characterized by different techniques such as FT-IR, SEM, and XRD. Then this adsorbent with maximum adsorption capacity of 52.40 mg g^{-1} was used as an effective and applicable adsorbent via DSPE-UV–Vis method for the extraction of AR as a food synthesis dye from environmental samples and its subsequent determination in them. Four effective factors on the extraction recovery, including eluent volume, pH, adsorbent dosage, and ultrasound time, as well as their interactions were evaluated and optimized by CCD-RSM as an effective mathematical tool. Based on CCD-RSM, the optimum conditions were achieved as follows: eluent volume = 0.3 (mL), pH = 3, adsorbent dosage = 10 (mg), and ultrasound time = 4.5 (min). Under optimum conditions, the validity and applicability of the present method were investigated in the presence of different interferences, such as metal ions and dye molecules and LOD of 26.0 ng mL^{-1}, LOQ of 75.0 ng mL^{-1}, and linear range of 80.0–5,000 ng mL^{-1} were achieved. The developed approach had the advantage of providing the highest efficiency of extraction associated with a lower consumption of the organic solvent (environmentally friendly) LOD, RSD%, and cost.

References

[1] E. Heidarizadi, R. Tabaraki, Simultaneous spectrophotometric determination of synthetic dyes in food samples after cloud point extraction using multiple response optimizations, Talanta, 148 (2016) 237–246.
[2] A. Ostovan, H. Asadollahzadeh, M. Ghaedi, Ultrasonically synthesis of Mn- and Cu-@ ZnS-NPs-AC based ultrasound assisted extraction procedure and validation of a spectrophotometric method for a rapid preconcentration of Allura Red AC (E129) in food and water samples, Ultrason. Sonochem., 43 (2018) 52–60.
[3] F. Mohammadi, A. Esrafili, M. Kermani, M. Behbahani, Application of modified magnetic nanoparticles with amine groups as an efficient solid sorbent for simultaneous

removal of 2,4-Dichlorophenoxyacetic acid and 2-methyl-4-chlorophenoxyacetic acid from aqueous solution: optimization and modeling, J. Iran. Chem. Soc., 15 (2018) 421–429.
[4] L. Yu, M. Shi, X. Yue, L. Qu, Detection of allura red based on the composite of poly (diallyldimethylammonium chloride) functionalized graphene and nickel nanoparticles modified electrode, Sens. Actuators, B, 225 (2016) 398–404.
[5] N. Pourreza, S. Rastegarzadeh, A. Larki, Determination of Allura red in food samples after cloud point extraction using mixed micelles, Food Chem., 126 (2011) 1465–1469.
[6] A. Jangju, K. Farhadi, M. Hatami, S. Amani, F. Esma-ali, A. Moshkabadi, F. Hajilari, Application of zein-modified magnetite nanoparticles in dispersive magnetic micro-solid-phase extraction of synthetic food dyes in foodstuffs, J. Sep. Sci., 40 (2017) 1343–1352.
[7] Y. Benmassaoud, M.J. Villaseñor, R. Salghi, S. Jodeh, M. Algarra, M. Zougagh, Á. Ríos, Magnetic/non-magnetic argan press cake nanocellulose for the selective extraction of sudan dyes in food samples prior to the determination by capillary liquid chromatograpy, Talanta, 166 (2017) 63–69.
[8] H. Filik, D. Giray, B. Ceylan, R. Apak, A novel fiber optic spectrophotometric determination of nitrite using Safranin O and cloud point extraction, Talanta, 85 (2011) 1818–1824.
[9] A. Ostovan, M. Ghaedi, M. Arabi, Q. Yang, J. Li, L. Chen, Hydrophilic multitemplate molecularly imprinted biopolymers based on a green synthesis strategy for determination of B-family vitamins, ACS Appl. Mater. Interfaces, 10 (2018) 4140–4150.
[10] M. Arabi, M. Ghaedi, A. Ostovan, Development of a lower toxic approach based on green synthesis of water-compatible molecularly imprinted nanoparticles for the extraction of hydrochlorothiazide from human urine, ACS Sustainable Chem. Eng., 5 (2017) 3775–3785.
[11] P. Toulabi, A. Daneshfar, R. Sahrai, Determination of hippuric acid in biological fluids using single drop liquid–liquid-liquid microextraction, Anal. Methods., 2 (2010) 564–569.
[12] A. Ostovan, M. Ghaedi, M. Arabi, A. Asfaram, Hollow porous molecularly imprinted polymer for highly selective clean-up followed by influential preconcentration of ultra-trace glibenclamide from bio-fluid, J. Chromatogr. A, 1520 (2017) 65–74.
[13] M. Behbahani, A. Veisi, F. Omidi, A. Noghrehabadi, A. Esrafili, M.H. Ebrahimi, Application of a dispersive micro-solid-phase extraction method for pre-concentration and ultra-trace determination of cadmium ions in water and biological samples, Appl. Organomet. Chem., 32 (2018) e4134.
[14] M.G. Kakavandi, M. Behbahani, F. Omidi, G. Hesam, Application of ultrasonic assisted-dispersive solid phase extraction based on ion-imprinted polymer nanoparticles for preconcentration and trace determination of lead ions in food and water samples, Food Anal. Methods, 10 (2017) 2454–2466.
[15] M. Behbahani, F. Omidi, M.G. Kakavandi, G. Hesam, Selective and sensitive determination of silver ions at trace levels based on ultrasonic-assisted dispersive solid-phase extraction using ion-imprinted polymer nanoparticles, Appl. Organomet. Chem., 31 (2017) e3758.
[16] M. Izanloo, A. Esrafili, M. Behbahani, M. Ghambarian, H.R. Sobhi, Trace quantification of selected sulfonamides in aqueous media by implementation of a new dispersive solid-phase extraction method using a nanomagnetic titanium dioxide graphene-based sorbent and HPLC-UV, J. Sep. Sci., 41 (2018) 910–917.
[17] M. Arabi, M. Ghaedi, A. Ostovan, Synthesis and application of in-situ molecularly imprinted silica monolithic in pipette-tip solid-phase microextraction for the separation and determination of gallic acid in orange juice samples, J. Chromatogr. B, 1048 (2017) 102–110.
[18] B. Socas-Rodríguez, J. Hernández-Borges, A.V. Herrera-Herrera, M.Á. Rodríguez-Delgado, Multiresidue analysis of oestrogenic compounds in cow, goat, sheep and human milk using core-shell polydopamine coated magnetic nanoparticles as extraction sorbent in micro-dispersive solid-phase extraction followed by ultra-high-performance liquid chromatography tandem mass spectrometry, Anal. Bioanal. Chem., 410 (2018) 2031–2042.
[19] M.A. Farooqui, P.S. Chauhan, P. Krishnamoorthy, J. Shaik, Extraction of silver nanoparticles from the leaf extracts of Clerodendrum inerme, Dig. J. Nanomater. Biostruct., 5 (2010) 43–49.
[20] M. Arabi, M. Ghaedi, A. Ostovan, Development of dummy molecularly imprinted based on functionalized silica nanoparticles for determination of acrylamide in processed food by matrix solid phase dispersion, Food Chem., 210 (2016) 78–84.
[21] M. Arabi, M. Ghaedi, A. Ostovan, Water compatible molecularly imprinted nanoparticles as a restricted access material for extraction of hippuric acid, a biological indicator of toluene exposure, from human urine, Microchim. Acta, 184 (2017) 879–887.
[22] C. Bendicho, C. Bendicho-Lavilla, I. Lavilla, Nanoparticle-assisted chemical speciation of trace elements, TrAC, Trends Anal. Chem., 77 (2016) 109–121.
[23] V. Zarezade, M. Behbahani, F. Omidi, H.S. Abandansari, G. Hesam, A new magnetic tailor made polymer for separation and trace determination of cadmium ions by flame atomic absorption spectrophotometry, RSC Adv., 6 (2016) 103499–103507.
[24] N. Rahbar, E. Behrouz, Z. Ramezani, One-step synthesis of zirconia and magnetite nanocomposite immobilized chitosan for micro-solid-phase extraction of organophosphorous pesticides from juice and water samples prior to gas chromatography/mass spectroscopy, Food Anal. Methods, 10 (2017) 2229–2240.
[25] V. Zarezade, A. Aliakbari, M. Es' haghi, M.M. Amini, M. Behbahani, F. Omidi, G. Hesam, Application of a new nanoporous sorbent for extraction and pre-concentration of lead and copper ions, Int. J. Environ. Anal. Chem., 97 (2017) 383–397.
[26] K.M. Dimpe, A. Mpupa, P.N. Nomngongo, Microwave assisted solid phase extraction for separation preconcentration sulfamethoxazole in wastewater using tyre based activated carbon as solid phase material prior to spectrophotometric determination, Spectrochim. Acta, Part A, 188 (2018) 341–348.
[27] O. Filippou, E.A. Deliyanni, V.F. Samanidou, Fabrication and evaluation of magnetic activated carbon as adsorbent for ultrasonic assisted magnetic solid phase dispersive extraction of bisphenol A from milk prior to high performance liquid chromatographic analysis with ultraviolet detection, J. Chromatogr. A, 1479 (2017) 20–31.
[28] M. Arabi, M. Ghaedi, A. Ostovan, S. Wang, Synthesis of lab-in-a-pipette-tip extraction using hydrophilic nano-sized dummy molecularly imprinted polymer for purification and analysis of prednisolone, J. Colloid Interface Sci., 480 (2016) 232–239.
[29] A. Keramat, R. Zare-Dorabei, Ultrasound-assisted dispersive magnetic solid phase extraction for preconcentration and determination of trace amount of Hg (II) ions from food samples and aqueous solution by magnetic graphene oxide (Fe_3O_4@ GO/2-PTSC): Central composite design optimization, Ultrason. Sonochem., 38 (2017) 421–429.
[30] F. Nemati, R. Zare-Dorabei, M. Hosseini, M.R. Ganjali, Fluorescence turn-on sensing of thiamine based on Arginine – functionalized graphene quantum dots (Arg-GQDs): Central composite design for process optimization, Sen. Actuators, B, 255 (2018) 2078–2085.
[31] M.S. Tehrani, R. Zare-Dorabei, Highly efficient simultaneous ultrasonic-assisted adsorption of methylene blue and rhodamine B onto metal organic framework MIL-68(Al): central composite design optimization, RSC Adv., 6 (2016) 27416–27425.
[32] R. Zare-Dorabei, S.M. Ferdowsi, A. Barzin, A. Tadjarodi, Highly efficient simultaneous ultrasonic-assisted adsorption of Pb(II), Cd(II), Ni(II) and Cu(II) ions from aqueous solutions by graphene oxide modified with 2,2′-dipyridylamine: Central composite design optimization, Ultrason. Sonochem., 32 (2016) 265–276.
[33] M.S. Tehrani, R. Zare-Dorabei, Competitive removal of hazardous dyes from aqueous solution by MIL-68(Al): derivative spectrophotometric method and response surface

methodology approach, Spectrochim. Acta, Part A, 160 (2016) 8–18.
[34] A. Tadjarodi, S.M. Ferdowsi, R. Zare-Dorabei, A. Barzin, Highly efficient ultrasonic-assisted removal of Hg(II) ions on graphene oxide modified with 2-pyridinecarboxaldehyde thiosemicarbazone: adsorption isotherms and kinetics studies, Ultrason. Sonochem., 33 (2016) 118–128.
[35] A.R. Bagheri, M. Ghaedi, A. Asfaram, S. Hajati, A.M. Ghaedi, A. Bazrafshan, M.R. Rahimi, Modeling and optimization of simultaneous removal of ternary dyes onto copper sulfide nanoparticles loaded on activated carbon using second-derivative spectrophotometry, J. Taiwan Inst. Chem. Eng., 65 (2016) 212–224.
[36] A. Ostovan, M. Ghaedi, M. Arabi, Fabrication of water-compatible superparamagnetic molecularly imprinted bio-polymer for clean separation of baclofen from bio-fluid samples: a mild and green approach, Talanta, 179 (2018) 760–768.
[37] S. Nipornram, W. Tochampa, P. Rattanatraiwong, R. Singanusong, Optimization of low power ultrasound-assisted extraction of phenolic compounds from mandarin (Citrus reticulata Blanco cv. Sainampueng) peel, Food Chem., 241 (2018) 338–345.
[38] R. Bandyopadhyaya, M.V. Sivaiah, P. Shankar, Silver-embedded granular activated carbon as an antibacterial medium for water purification, J. Chem. Technol. Biotechnol., 83 (2008) 1177–1180.
[39] X. Yin, L. Song, X. Xie, Y. Zhou, Y. Guan, J. Xiong, Preparation of the flexible ZrO_2/C composite nanofibrous film via electrospinning, Appl. Phys. A, 122 (2016) 678.
[40] Y. Zhang, L. Guo, X. Zhao, C. Wang, F. Ye, Toughening effect of Yb_2O_3 stabilized ZrO_2 doped in $Gd_2Zr_2O_7$ ceramic for thermal barrier coatings, Mater Sci. Eng., A, 648 (2015) 385–391.
[41] H.A. Oualid, Y. Essamlali, O. Amadine, K. Daanoun, M. Zahouily, Green synthesis of Ag/ZnO nanohybrid using sodium alginate gelation method, Ceram. Int., 43 (2017) 13786–13790.
[42] K. Dhanalekshmi, K. Meena, DNA intercalation studies and antimicrobial activity of Ag@ZrO_2 core–shell nanoparticles in vitro, Mater Sci. Eng. C., 59 (2016) 1063–1068.
[43] F. Mohammadi, A. Esrafili, H.R. Sobhi, M. Behbahani, M. Kermani, E. Asgari, Z.R. Fasih, Evaluation of adsorption and removal of methylparaben from aqueous solutions using amino-functionalized magnetic nanoparticles as an efficient adsorbent: optimization and modeling by response surface methodology (RSM), Desal. Wat. Treat., 103 (2018) 248–260.
[44] I. Langmuir, The adsorption of gases on plane surfaces of glass, mica and platinum, J. Am. Chem. Soc., 40 (1918) 1361–1403.
[45] A.R. Bagheri, M. Ghaedi, A. Asfaram, A.A. Bazrafshan, R. Jannesar, Comparative study on ultrasonic assisted adsorption of dyes from single system onto Fe_3O_4 magnetite nanoparticles loaded on activated carbon: experimental design methodology, Ultrason. Sonochem., 34 (2017) 294–304.
[46] A.T. Bisgin, M. Ucan, I. Narin, Comparison of column solid-phase extraction procedures for spectrophotometric determination of E129 (Allura Red) in foodstuff, pharmaceutical, and energy drink samples, J. AOAC Int., 98 (2015) 946–952.
[47] S. Bonan, G. Fedrizzi, S. Menotta, C. Elisabetta, Simultaneous determination of synthetic dyes in foodstuffs and beverages by high-performance liquid chromatography coupled with diode-array detector, Dyes Pigm., 99 (2013) 36–40.
[48] F. Turak, M.U. Ozgur, Simultaneous determination of Allura Red and Ponceau 4R in Drinks with the use of four derivative spectrophotometric methods and comparison with high-performance liquid chromatography, J. AOAC Int., 96 (2013) 1377–1386.
[49] Z. Fan, Y. Yu, Magnetic solid-phase extraction coupled with HPLC for the determination of Allura Red in food and beverage samples, Food Addit. Contam., 33 (2016) 1527–1534.
[50] A. Asfaram, M. Ghaedi, H. Abidi, H. Javadian, M. Zoladl, F. Sadeghfar, Synthesis of Fe_3O_4@CuS@Ni_2P-CNTs magnetic nanocomposite for sonochemical-assisted sorption and preconcentration of trace Allura Red from aqueous samples prior to HPLC-UV detection: CCD-RSM design, Ultrason. Sonochem., 44 (2018) 240–250.
[51] Y.E. Unsal, M. Tuzen, M. Soylak, Spectrophotometric determination of trace levels of allura red in water samples after separation and preconcentration, Food Chem. Toxicol., 49 (2011) 1183–1187.